ISBN: 978-3-95450-208-0 doi:10.18429/JACoW-IPAC2019-THPMP047

ADVANCED MODELING AND OPTIMIZATION OF THERMIONIC ENERGY CONVERTERS *

J. P. Edelen†, N. M. Cook, C. C. Hall, Y. Hu, RadiaSoft LLC, 80301, Boulder, CO, USA
J.-L. Vay, LBNL, Berkeley, CA, USA

Abstract

Thermionic energy converters (TEC) are a class of thermoelectric devices, which promise improvements to the efficiency and cost of both small- and large-scale electricity generation. A TEC is comprised of a narrowly-separated thermionic emitter and an anode. Simple structures are often space-charge limited as operating temperatures produce currents exceeding the Child-Langmuir limit. We present results from 3D simulations of these devices using the particle-in-cell code Warp, developed at Lawrence Berkeley National Lab. We demonstrate improvements to the Warp code permitting high fidelity simulations of complex device geometries. These improvements include modeling of non-conformal geometries using mesh refinement and cut-cells with a dielectric solver, in addition to importing geometries directly from standard CAD output. In this paper we showcase some of these new features and demonstrate their use.

INTRODUCTION

Thermionic energy converters (TECs) operate by using an external heat source to drive thermionic emission of electrons across a narrow vacuum to be collected on an opposing conductor. A traditional TEC is comprised of narrowly separated plates; thermionic emission at the cathode releases electrons which travel to the anode, producing a current which may generate electrical power [1, 2]. To overcome space charge limitations an accelerating grid can be used to boost the amount of current that can be extracted. A magnetic field may be added to constrain electron trajectories and limit losses on the grid.

Modeling complex devices such as these is challenging; Warp [3] is a fully 3D particle in cell code capable of handling a wide range of physics problems and is well suited to modeling TECs. However, the interface to Warp makes rapid prototyping difficult and many of Warp's features have not been tested on problems relevant to TECs. Over the past two years we have constructed a graphical interface to Warp deployed in the cloud computing framework Sirepo [4]. This interface allows users to work with the code without needing to modify underlying Python scripts. Here we detail a couple of recent improvements to this interface that allow for the direct import of complicated 3-D CAD geometries and advanced visualization of impact densities on objects inside the simulations.

* This material is based upon work supported by the U.S. Department of Energy, Office of Science, Office of High Energy Physics under Award Number DE-SC0017162.
† jedelen@radiasoft.net

Additionally we have been testing Warp's physics engine on problems of interest for TECs. Specifically self consistent emission models and shaped emitters in order to accurately simulate relevant cathode configurations. In this paper we detail recent efforts to apply mesh refinement for accurate modeling of shaped emitters and emitter arrays.

INTERFACE IMPROVEMENTS FOR WARP

New CAD Interface

We have developed a Python CAD module capable of handling arbitrary geometries in our open-source framework. This new CAD module takes advantage of the open-source Python library PyMesh[1] to prototype the creation, manipulation, and I/O of 3D mesh configurations defined in a CAD export file. PyMesh supports parsing the following formats: .obj, .ply, .off, .stl, .mesh, .node, .poly and .msh. Two efficient and robust ray-mesh intersection finding algorithms have been implemented in the new CAD module. The ray-mesh intersection finding routine is needed by Warp to solve the Poisson's equation. It is also necessary to evaluate particle-grid interaction with high accuracy.

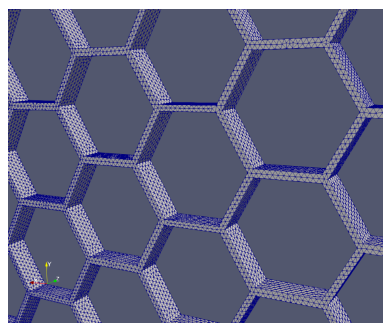

Figure 1: Geometry of the honeycomb grid as generated by comsol.

Our implementation has been tested using grids with complex geometries generated using the COMSOL Multiphysics application. Figure 1 shows the representation of a grid with honeycomb geometry defined in an STL format. This modified CAD module can import STL files, compute surfaces and intercepts with Warp's underlying solver mesh, and pass the resulting information to Warp's solver and particle scraper. Figure 2 shows the total electric field for a transverse cross-section of the honeycomb grid obtained from Warp's multi grid Poisson's solver.

[1] https://github.com/PyMesh/PyMesh

ISBN: 978-3-95450-208-0 doi:10.18429/JACoW-IPAC2019-THPMP047

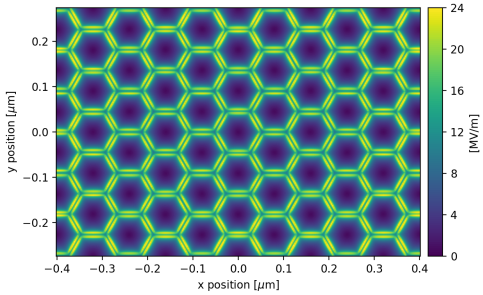

Figure 2: Electric field at a slice of the honey-comb grid that was imported using an stl file.

Advanced Visualizations

We have also developed an Impact Density diagnostic that allows users to see where particles intersect3D objects in the simulation. The diagnostic supports arbitrary, convex conductor shapes, using a VTK-based visualization pipeline commensurate with the Sirepo interface. To support arbitrary geometries in 2D and 3D, Delaunay triangulation was used to reproduce the surfaces. Figure 3 illustrates the diagnostic output for an arbitrary collection of shapes.

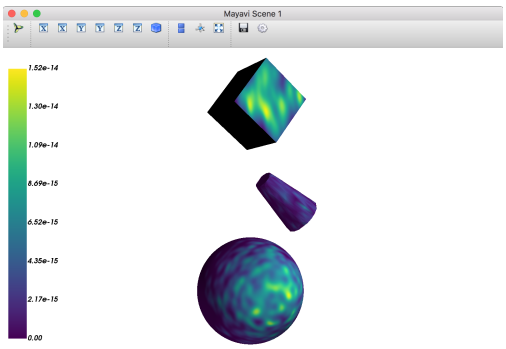

Figure 3: Example of the impact density on several types of objects. This diagnostic will be available in Sirepo.

MODELING SHAPED EMITTERS

Shaped emitters are of interest for thermionic energy converters because of the ability to enhance the emission at specific locations that allow for fewer particles to intersect the grid. Sufficient field enhancement can enable the cathode can operate at a higher temperature thereby increasing the efficiency of the device. To study the effectiveness of Warp for modeling shaped emitters we consider the field solution for a single conical emitter tip followed by a small array of conical emitter tips. We then simulate field-enhanced thermionic emission for a single emitter tip.

Field Solution

First we examine a single emitter tip located on the beam axis and vary the mesh refinement parameters. Figure 4 shows the total field for a slice of the simulation that intersects the emitter tip.

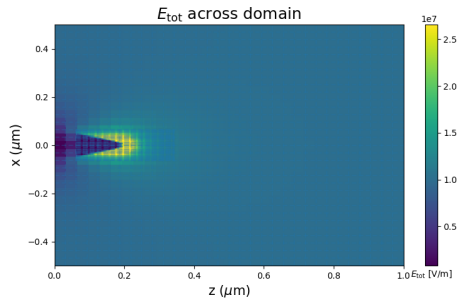

Figure 4: Contour plot of the total field as a function of x and z for a single emitter. The grid is superimposed on the plot showing the mesh refinement patch.

Figure 5 shows the longitudinal field as a function of position as we vary the density of the mesh refinement patch for two different global mesh densities. Top is a 16x16x16 grid and bottom is a 32x32x32 grid. The vertical dashed line represents the surface of the cathode. As expected, as we increase the density of the mesh refinement patch the field solution converges. When using a coarser global mesh there is a kink in the field at around 3μm. This kink results from a coarse global mesh intersecting with a fine local mesh.

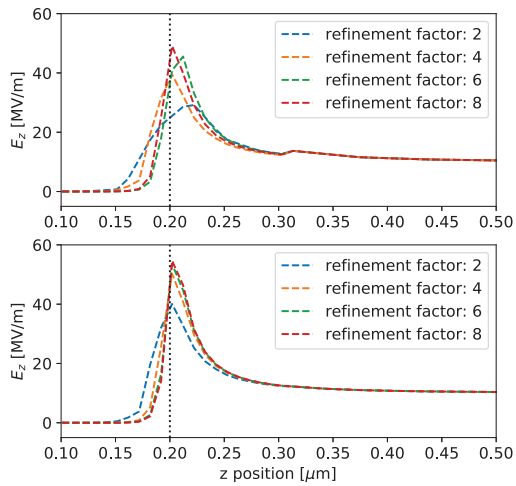

Figure 5: Comparison of the field solution on axis for different degrees of mesh refinement. Top is for a 16x16x16 grid and bottom is for a 32x32x32 grid.

Next we consider an array of emitters and study how different mesh refinement schemes affect the fields on the emitter tips and between the emitters. Figure 6 shows a contour plot of the fields for a 4 tip array which highlights the geometry we are simulating.

We studied different mesh-refinement configurations including: 1) no refinement between the tips, 2) refinement on the tips and between the emitters, or 3) one large refinement patch covering the emitter array. Figure 7 shows the total field as a function of longitudinal position both on the emitter tip and between two emitters for the different mesh refine-

ISBN: 978-3-95450-208-0 doi:10.18429/JACoW-IPAC2019-THPMP047

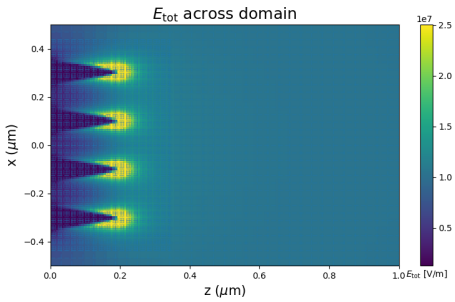

Figure 6: Contour plot of the total field as a function of x and z for an emitter array. The grid is superimposed on the plot showing the mesh refinement patch.

ment configurations. Here we see very little dependance of the fields on the level of refinement.

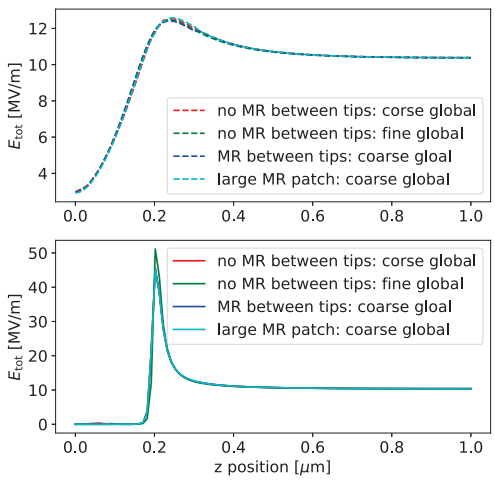

Figure 7: Comparison of fields on axis (left axis dashed lines) and on the emitter tips (right solid lines) for different mesh refinement configurations. Note that there is very little dependance of the fields to the mesh refinement schemes.

However if we examine the field along a transverse slice that intersects the emitters we see a strong dependence on the different mesh refinement configurations. Figure 8 shows the total field as a function of transverse position. The blue and orange lines have no refinement between the emitters, the red and green lines have mesh refinement between the emitters. Here we can clearly see that additional mesh refinement between the emitters affects the field close to the emitter surface however the fields between emitters is relatively unchanged. Note that the field goes to zero inside the emitter tips.

Emission Model and Simulations

Next we consider emission from these surfaces. To model this we define a custom emitter class that collects the fields on the surface of the cathode at each time-step. Given this field,

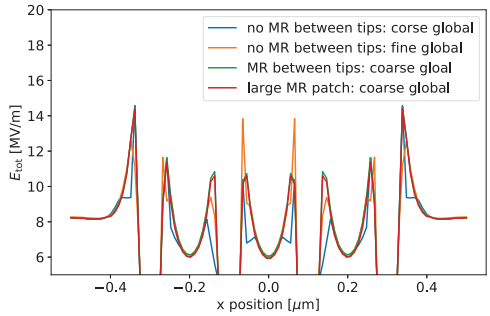

Figure 8: Comparison of total field as a function of transverse position along the emitter array. Here we can see a strong dependence of the fields on the mesh refinement configuration.

the emitter injects current using the Richardson-Dushman equation with a Schottky correction, Eq. (1).

$$J = A_g T^2 \exp \frac{-(W - \Delta W)}{k_b T} \tag{1}$$

where ΔW is the Schottky correction for the work function defined by $\Delta W = \sqrt{\frac{q^3 E}{4\pi\epsilon_0}}$. Because the electric field on the surface of the emitter is normal to the surface, we compute the total field on the surface at a given emission site for the Schottky correction. From here we compute the effective work function at the emission site and inject the appropriate number of particles given a pre-defined particle weight. Using this model we will simulate the emission well below the space-charge limit and study field enhancement and the onset of space-charge limited emission.

CONCLUSION

In conclusion, we have further improved and tested our browser based interface to Warp. This includes more a robust CAD import module, advanced diagnostics such as 3-D impact density visualization tools, and a prototype optimization framework. We have also verified mesh-refinement tools for modeling of shaped emitters and begun study of these emitters in Warp.

REFERENCES

[1] A. Schock, "Optimization of Emission-Limited Thermionic Generators", in *Journal of Applied Physics* , vol. 32, p. 1564, 1961.

[2] S. Meir et al., "Highly-efficient thermoelectronic conversion of solar energy and heat into electric power", in *Journal of Renewable and Sustainable Energy*, vol. 5, p. 043127, 2013.

[3] J.-L. Vay et al., "Novel methods in the Particle-In-Cell accelerator Code-Framework Warp", in *Computational Science & Discovery*, vol. 5, p. 014019, 2012.

[4] N. M. Cook, J. P. Edelen, C. C. Hall, and J.-L. Vay, "Self-Consistent Simulation and Optimization of Space-Charge Limited Thermionic Energy Converters", in *Proc. 9th Int. Particle Accelerator Conf. (IPAC'18)*, Vancouver, Canada, Apr.-May 2018, pp. 543–545. doi:10.18429/JACoW-IPAC2018-MOPML060